

Study of Intense Geomagnetic Storms and Their Possible Effects on Society

G. S. LAKHINA, G. JADHAV, S. ALEX, AND AJAY DHAR
Indian Institute of Geomagnetism, Navi Mumbai
E-mail: lakhina@iig.res.in

Abstract

Intense geomagnetic storms form an important component of Space Weather. We have analyzed some intense geomagnetic storms with $Dst < -100$ nT that occurred during 1998-2001. We made use of the ground magnetic data from the Alibag (Geog. $18^{\circ} 37' N, 72^{\circ} 52' E$, Geomag. $10^{\circ} N, 145^{\circ} 9'$) and high latitude station, Maitri, Antarctica (Geog. $70^{\circ} 46' S, 11^{\circ} 44' E$, Geomag. $62^{\circ} 8' S, 52^{\circ} 8'$). In addition, the magnetic field and plasma data from the NASA's Advanced Composition Explorer (ACE) spacecraft has been used to find the effects of interplanetary parameters that cause intense storm. Geomagnetic indices, like, disturbance storm time (Dst) index and auroral electrojet (AE) index are used to compute the energy budget of the intense storms. Some of the adverse effects of intense and super-intense geomagnetic storms on telecommunication, navigation, and on spacecraft functioning that directly affect the modern society are discussed.

Introduction

The Geomagnetic field protects the Earth from cosmic rays (the high energy particles coming from the Galaxy) and solar wind (the ionized gas or plasma flowing out of the Sun) just like a barrier.

Without this magnetic field barrier, the solar wind could blow away the atmosphere of the Earth, and the cosmic rays might have destroyed our optic nerve system and mutated our cells leading to the extinction of life on the Earth.

The study of Geomagnetism is, therefore, directly linked to survival of human and other species on the Earth.

The Sun is emitting solar wind all the time. At the Earth's orbit, the solar wind has density of about 5 particles cm^{-3} , and speeds of ~ 400 km s^{-1} . Both density and velocities are variable, and the speeds can exceed 1500 km s^{-1} during high speed streams. The interaction of the solar wind with the geomagnetic field leads to the formation of the magnetosphere. Because of this interaction, the magnetic field on the dayside is compressed where as on the nightside it is stretched in the form of long tail, just like a comet. Figure 1 shows a schematic view of the Earth's magnetosphere along with several current systems, which

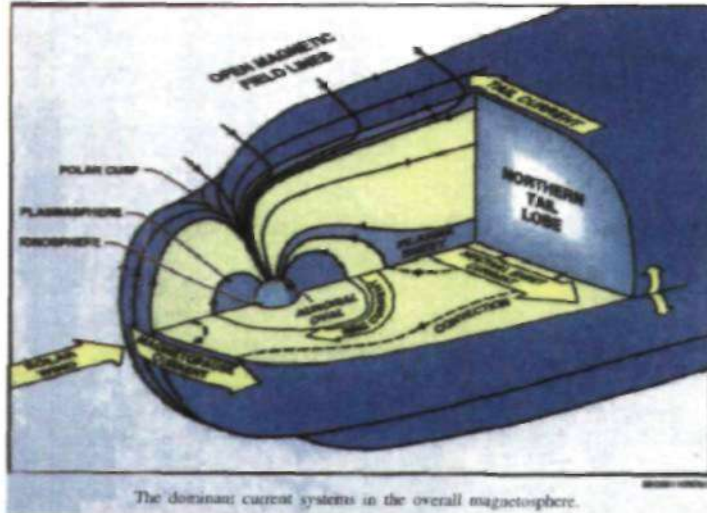


Fig.1. Schematics of the three dimensional view of the Earth's magnetosphere and its various current systems. The magnetosphere is formed during the interaction of solar wind with the geomagnetic field.

help to redistribute and dissipate the solar wind energy transferred to the magnetosphere. Magnetopause boundary separates the plasma and fields connected to the geospace and the interplanetary medium.

Periodically the Sun becomes highly eruptive, for example, solar flares event are the mightiest eruptions from the tenuous atmosphere of the Sun that predominantly occur when large scale changes in the solar magnetic field take place during the high solar activity periods. Often, following the explosion in the Sun's surface an eruption of a cloud of electrified magnetic gas, called coronal mass ejection (CME), is hurled in space from the solar corona. Both the solar flare ejecta and the CMEs carry dense plasma blobs traveling at speeds extending up to 2000 km s^{-1} . The solar wind-magnetosphere coupling is greatly enhanced when the CMEs, or the solar flare ejecta, or the fast streams from the coronal holes, that are accompanied by long intervals of southward interplanetary magnetic field (IMF) as in a "magnetic cloud" (Klein and Burlaga, 1982), impinge on the Earth's magnetosphere. This situation, generally, leads to the occurrence of a geomagnetic magnetic storm which is characterized by a main phase during which the horizontal component of the Earth's low-latitude magnetic field is significantly depressed over a time span of one to a few hours. This is followed by a recovery phase which may extend for ~ 10 hrs or more (Rostoker, 1997). The intensity of a geomagnetic storm is measured in terms of the disturbance storm time index (Dst). Magnetic storms with $\text{Dst} < -100 \text{ nT}$

are called intense and those with $Dst < -500$ nT are called super-intense. During magnetic storms a large amount of energy is dissipated in the Polar Regions, leading to profound changes in the global morphology of the upper atmosphere. The storm is generally accompanied by large bright auroral brightening; occasionally they are seen to move equator-ward from their usual location (known as expansion of the auroral oval), and could be seen at sub-auroral to mid-latitude locations.

The main mechanism of energy transfer from the solar wind to the Earth's magnetosphere is believed to be the magnetic reconnection (Dungey, 1961). The efficiency of the reconnection process is considerably enhanced during southward interplanetary magnetic field (IMF) intervals (Gonzalez and Tsurutani, 1987; Gonzalez et al., 1989; Tsurutani and Gonzalez, 1997; Tsurutani et al., 1999). This leads to strong plasma injection from the magnetotail towards the inner magnetosphere causing intense auroras at high-latitude nightside regions. The impulsive release of stored magnetotail energy gives rise to the phenomenon of substorm. Further, as the magnetotail plasma gets injected into the nightside magnetosphere, the energetic protons drift to the west and electrons to the east, forming a ring of current around the Earth. This current, called the "ring current", causes a diamagnetic decrease in the Earth's magnetic field measured at near-equatorial magnetic stations, as shown in Figure 2. The decrease in the equatorial magnetic field strength, measured by the Dst index, is directly related

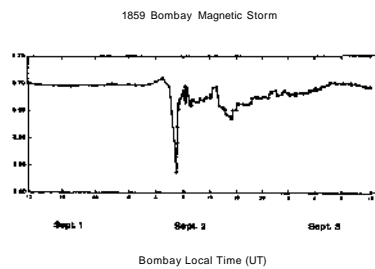


Fig. 2. Calaba magnetogram for the historical September 2, 1859 super intense magnetic storm. Solar flare ejecta/CME was the cause of this super magnetic storm with $Dst \sim -1600$ nT.

to the total kinetic energy of the ring current particles (Dessler and Parker 1959; Sckopke 1966). Hence the Dst index is considered as a good measure of the energetics of the magnetic storm. The Dst index itself is influenced by the interplanetary parameters (Burton et al. 1975). The key processes leading to geomagnetic storms are shown in Fig. 3. (Lakhina and Alex 2002).

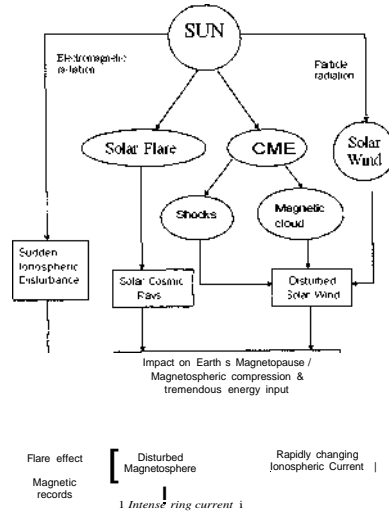


Figure 3 Geomagnetic storms recorded at Magnetic Observatories

Fig 3 Schematics of the key processes leading to intense geomagnetic storms

Here we study energetics of 9 intense geomagnetic storms (all with $Dst < -175$ nT) that occurred during the period 1998 - 2001, using the ground magnetic data from Alibag (Geog. $18^{\circ} 37' N, 72^{\circ} 52' E$, Geomag. $10^{\circ} N, 145^{\circ} 9'$) Magnetic Observatory and Maitri (Geog. $70^{\circ} 46' S, 111^{\circ} 44' E$, Geomag. $62^{\circ} S, 52^{\circ} 8'$) station at Antarctica. Some effects of the intense storms on society are also discussed.

Methodology

The study is mainly focused on the ground magnetic signatures as observed from the digital magnetic data from the low latitude observatory, Alibag and the high latitude observatory, Maitri, Antarctica. In addition, we make use of the plasma and magnetic field data from the NASA's Advanced Composition Explorer (ACE) spacecraft to investigate the effects of interplanetary parameters that cause intense storm. Where as the magnetic observatories at low-latitudes are well suited for the study of magnetic storms, the Maitri, the Indian magnetic station at Antarctica, is ideal for the study of sub storm phenomena and magnetosphere-ionosphere coupling. Further, we use geomagnetic indices, like, Dst index and AE index, to compute the energy budget of the intense storms (see Jadhav et al., 2004, for details). The list of 9 storms selected for this study is given in Table 1.

Sr. No.	Date	Dst^* mm (nT)	Comments
1	4 May 98	-230	No Initial phase
2	25 Sep 98	-206	Magnetic Cloud
3	22 Sep 99	-178	Long Initial phase (7 hr)
4	22 Oct 99	-266	SSC is seen ~22 hr before storm development
5	6 Apr 00	-314	Magnetic Cloud
6	12 Aug 00	-239	Magnetic Cloud
7	17 Sep 00	-226	Disturbed before onset of the storm
8	31 Mar 01	-381	Two-step storm
9	11 Apr 01	-259	Magnetic Cloud

Table 1: Shows the list of 9 intense magnetic storms selected for this study. The Dst^* stands for the pressure corrected Dst index.

Some case studies

a) October 22, 1999:

A very intense magnetic storm with $Dst = -266$ nT was recorded on this day. Interplanetary parameters and the associated ground magnetic signatures observed from the low latitude (one minute digital records from Alibag) and high latitude (30 seconds digital records from Maitri) geomagnetic field variations for this intense storm are shown in Figure. 4. The magnetic field variations of



Fig. 4. Ground magnetic field observation at Alibag and Maitri, along with interplanetary magnetic field (B_y and B_z components), the AE and Kp indices for the storm taking place on October 22, 1999. Prolonged southward conditions of B_z is the salient feature of the event with multiple substorm occurrence as is evident from the variations at Maitri.

the H-component at Alibag and the variations of the X-component ($X = H \cos D$) and Y-component ($Y = H \sin D$) at Maitri are shown in the upper panel of this figure. Maitri being an auroral zone station, it is preferable to use the X-component rather than the H-component, due to large D variation. Histograms of Kp and AE index shown for the event clearly depict the magnitude of the storm effect in the magnetosphere. Kp index reached a value of 8 during the period of main phase and coincided with the large values of AE. The main phase of the magnetic storm started after the southward turning of the interplanetary magnetic field around 2200 UT on 21 October with a prominent southward turning of B_z for more than 8 hours (i.e., B_z becoming negative). During the main phase interval, multiple peak structures are observed in Alibag and Maitri data. The Maitri data shows intense substorm activity. The Riometer data from Maitri showed strong ionospheric radio absorption coincident with field-aligned current enhancements (not shown here) (Rajaram et al., 2001). The Kp index remained high during the recovery phase. This intense magnetic storm has a long initial phase as the ring current developed ~ 22 hours after the occurrence of storm sudden commencement (SSC) (not shown).

b) September 22, 1999:

Figure 5 shows the ground magnetic and geomagnetic activity index data in the same format of Figure 4. Here also, the main phase of the magnetic storm started after the B_z component became negative around 19:30 UT and persisted for nearly 5 hours. This magnetic storm has $Dst = -178$ nT and a relatively short recovery phase. Both X and Y components of the Maitri magnetic field show intense substorm activity correlated with the AE index at 2100 UT on 22 September and 0430 UT on 23 September. The dominance of field aligned currents (FACs) is manifested in the large fluctuations as observed in the variations of X and Y-components at Maitri.

c) March 31, 2001:

This magnetic storm was very intense with $Dst = -381$ nT. The Kp index remained high (i.e., $Kp > 6$) for almost a full day, with two distinct peaks. The variations in the H-component at Alibag for the day have shown the characteristics of a two-step storm (Kamide et al., 1988). The Maitri data shows intense substorm activity following enhanced field-aligned currents (FAC). The first main phase started after B_z became negative around 0430 UT on 31 March and ended near 0730 UT. The recovery phase began when B_z started becoming less negative. However, the onset of the second main phase is evident when B_z again became negative from 1600 UT and stayed negative for some time. During the 1st main phase, Maitri has loss of data. During the second main phase period, intense substorm activity is clearly seen from the variations in X and Y-component data at Maitri, which has a good correlation with the fluctuating AE

Thus the contribution from FACs during the substorm activity is distinctly evident at Maitri for this event

22 sep 99

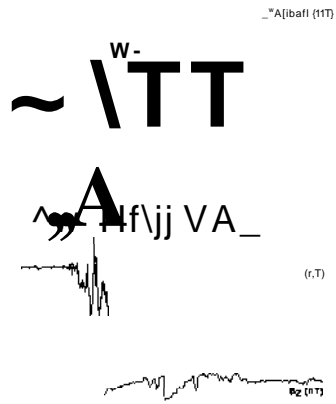


Fig. 5 . Geomagnetic variations at Maitri and at Alibag for the storm event of September 22, 1999 .Substorm activity seen in the X and Y components at Maitri on 22 September 22 and 23 is seen to coincide with the southward B z.

Energy Budget



$$\int_{-1}^1 J_{jvmk}^1$$

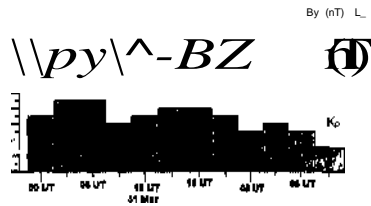


Fig. 6. Geomagnetic field variations at Alibag and Maitri for the intense storm of March 31, 2001. This is a two step storm. Prior to the onset of the first main phase on 31 March, correspondence between the fluctuating B_z and the initial phase pattern is clear from the variations of Halibag. The magnetic data from the Maitri station was not available during the first step of the storm.

We have computed various components of magnetospheric and ionospheric energies involved during the occurrence of magnetic storms. The energies in the units of Joules are obtained through the time integration of the energy rates. In order to estimate the total energy input to the magnetosphere (EM), we have used epsilon parameter, ϵ , defined by Perreault and Akasofu (1978),

$$\epsilon = V_{sw} B^2 L_0^2 \sin^2 \theta \quad (1)$$

where B is the magnitude of the interplanetary magnetic field (IMF), θ is the angle between the geomagnetic field vector and the IMF vector at the front of the magnetosphere in the equatorial plane, and L_0 is the radius of the dayside magnetopause. Here L_0 is taken as the Chapman-Ferraro magnetopause distance (L_{CF}), which is obtained from the balance between the solar wind plasma pressure and the magnetic pressure (Sibeck et al, 1991; Mac-Mahon and Gonzalez 1997). The above expression shows that even under weakly northward MF conditions, still significant energy coupling is possible.

Further, the total kinetic energy of solar wind is denoted by E_{sw} , whereas ionospheric dissipated energies due to joule heating, auroral particle precipitation and ring current are denoted by E_j , E_A and E_{RC} , respectively. The total energy dissipated, E_t , is the sum of E_j , E_A , and E_{RC} . Note that the quantities E_j and E_A are for one hemisphere only. We have used the empirical formulae given by Akasofu (1981a,b) to compute the energy dissipated by Joule heating (E_j) and auroral particle precipitation (E_A). The ring current energy dissipation is calculated combining the energy balance equation with Dessler-Parker-Sckopke (DPS) relationship (Dessler and Parker, 1959; Sckopke, 1966; Liemohn et al. 1999; Ebihara and Ejiri, 2000).

Table 2 shows the energy budget for all the 9 geomagnetic storms taking into account the main phase of the storm (the recovery phase period is neglected) only.

Event	E_{sw}	E_j	E_A	RC	EM	$E_t = E_j + E_A + RC$
May 4, 98	1986	1.82	0.91	7.73	71.7	10.46
Sep 25, 98	2390	5.29	2.64	14.06	147	21.99
Sep 22, 99	874	1.36	0.68	8.19	24.4	10.23
Oct 22, 99	1946	3.46	1.73	14.81	182	19.99

Apr 6, 00	3825	3.83	1.91	17.99	165	23.73
Aug 12, 00	1858	4.6	2.3	13.57	232	20.47
Sep 17, 00	3231	2.71	1.36	11.10	66.6	15.17
Mar 31, 01	3871	2.28	1.14	1918	201	22.60
Apr 11, 01	7201	5.8	2.9	15.01	159	23.71
Average	3020	3.46	1.73	13.51	138.7	18.70

Table 2: Energy budget during main phase of the storm. Energies are expressed in 10^{15} J.

From Table 2, it is clear that during the main phase of the storm, the energy available in the solar wind ranges from 9×10^{17} to 39×10^{17} J and the average is 30×10^{17} J (cf. 2nd column). This is in fair agreement with the estimates of Feldstein et al. [2003], but about 50% lower than the values obtained by MacMahon and Gonzalez [1997]. The mean of the energy transferred into the magnetosphere comes to $\sim 140 \times 10^{15}$ J (cf. 6th column), which is in good agreement with the estimates given in above-mentioned papers. The energy dissipated in the auroral ionosphere (4th column) and through Joule heating (3rd column) varies between $(1 - 6) \times 10^{15}$ J. The ring current energy dissipation (5th column) ranges from $8 - 19 \times 10^{15}$ J, with an average of 13.5×10^{15} J. Therefore, roughly 5% of total solar wind kinetic energy is available for the redistribution in the magnetosphere. It is noted that about 13.5% of magnetospheric energy goes into the auroral dissipation, Joule heating (one hemisphere) and ring current; the estimation turns to 18% by considering the energy dissipated in both the hemispheres. The comparison of the energy estimates from various previous studies have been done by Feldstein et al. [2003] and it is found that they are pretty contradictory to each other.

We have computed the energy budget for the above 9 storms taking into consideration the total storm period consisting of the main phase and the recovery phase. In the present study, we consider the recovery phase to end at a time when derivative of Dst with respect to time is significantly small, rather than when Dst reaches exactly to its pre-storm value. The results are shown in Table 3.

Event	E_{sw}	E_j	E_A	E_{RC}	E_M	$E_T = E_j + E_A + E_{RC}$
May 4, 98	8490	9.29	4.64	15.46	177	29.39
Sept 25, 98	4548	14.4	7.21	15.76	261.5	37.37
Sep 22, 99	5131	5.02	2.51	14.12	73	21.65
Oct 22, 99	4781	8.83	4.42	19.92	215	33.17
Apr 6, 00	7488	6.68	3.34	25.12	193	35.14
Aug 12, 00	5464	12.4	6.21	19.03	382	37.63
Sept 17, 00	12440	6.05	3.03	16.5	94.7	25.58
Mar 31, 01	13752	12.7	6.35	39.99	562	59.04
Apr 11, 01	8780	10.6	5.31	20.37	272	36.27
Average	7874.9	9.55	4.78	20.69	247.8	35.02

Table 3: representing the energy budget for the total storm period with energies expressed in unit of 10^{15} J.

From Table 3, it is noted that, for the total storm period, the energy dissipated through the particle precipitation in the auroral ionosphere varies from $3-7 \times 10^{15}$ J (4th column), whereas that for Joule heating ranges from $5-14 \times 10^{15}$ J (3rd column). Ring current energy estimates vary between $14-40 \times 10^{15}$ J (5th column), with an average of 21×10^{15} J. About 3.5% of E_{sw} (2nd column) is available for the redistribution in the magnetosphere and around 20% of E_M (6th column) goes into total magnetospheric energy consumption in both the hemispheres. The differences between E_M and E_T could be attributed to the energy consumption in the magnetospheric tail current and the field-aligned current. Wide range of energies stored in various parts of the magnetosphere indicates that though all the storms fall in the same category of 'intense storms', each event involves different energy budget. This further suggests that the nature of the magnetospheric response during storm time depends on the conditions of solar ejecta substantially.

Magnetic Storms and Society

Modern society is becoming ever increasingly dependent on space technology for daily routine functions, such as communication, navigation, data transmission, global surveillance of resource surveys, atmospheric weather, etc. Space weather refers to conditions on the Sun and in the solar wind,

magnetosphere, ionosphere, and thermosphere that can influence the performance and reliability of space-borne and ground-based technological systems and can endanger human life or health.

Intense and super-intense geomagnetic storms create hostile space weather conditions that can generate many hazards to the spacecraft as well as technological systems at ground.

Geomagnetic storms can cause life-threatening power outages such as Hydro Quebec power failure during March 1989 magnetic storm. In the magnetosphere, fluxes of relativistic electrons increase many folds during intense storms and it can lead to malfunctioning and failure of satellite instruments due to deep dielectric charging. During the past decade alone, many spacecraft malfunctioned for several hours or even were permanently damaged due to adverse space weather conditions during intense geomagnetic storms. Strong Geomagnetically induced currents (GICs) produced by sudden short-period variations in the geomagnetic field during intense magnetic storms can cause damage to power transmission lines and corrode long pipelines.

Intense and super-intense geomagnetic storms produce disturbances in the ionosphere-thermosphere system that can cause communication failure and navigational errors. Heating and subsequent expansion of the thermosphere during such storms could produce extra drag on the low earth orbiting satellites that could reduce their lifetimes significantly. Super-intense geomagnetic storms like the 1 - 2 September 1859 event, if they were to occur today would produce adverse space weather conditions on a much larger scale than the intense storm of March 1989 with catastrophic consequences for the society (Tsurutani et al. 2003).

Conclusion

During Main phase of the storm, almost 5% of the total solar wind kinetic energy is available for redistribution in the magnetosphere, whereas during total storm period it reduces to 3.5%. All 9 intense magnetic storms occurred during the period of southward IMF.

The Maitri station data clearly shows the correlation between the substorm activity and the southward component of IMF. Adverse space weather conditions created by intense and super-intense magnetic storms could affect communication, navigation and proper functioning as well as the life span of the technological systems in space.

Acknowledgement

Some portions of the work were done while G. S. Lakhina was visiting Solar Terrestrial Environment Laboratory (STEL), Nagoya University, Toyokawa,

Japan. He would like to thank Prof. Y. Kamide for the kind hospitality. The authors are grateful to NSSDC at Goddard Space Flight Center for making available the ACE satellite measurements. We thank the ACE SWEPAM instrument team, ACE Magnetic Field instrument team and the ACE Science Center for providing the ACE data. We are also thankful to WDC-C2, Kyoto, for supplying Dst and SymH indices. We acknowledge the organizational and logistic support provided by Department of Ocean Development, Govt of India, for carrying out Geomagnetic studies at Antarctica.

References

- AKASOFU, S. I. (1981a) Energy coupling between the solar wind and the magnetosphere. *Space Sci. Rev.*, v. 28, pp.121-190.
- AKASOFU, S. I. (1981b) Relationship between AE and Dst indices during geomagnetic storms. *J. Geophys. Res.*, v. 86, pp. 4820.
- BURTON, R.K., MCPHERSON, R. L. and RUSSELL, C. T. (1975) An empirical relationship between interplanetary conditions and Dst. *J. Geophys. Res.*, v. 80, pp.4204-4214.
- DESSLER, A.J. and PARKER, E. N. (1959) Hydromagnetic theory of magnetic storms. *J. Geophys. Res.*, v. 64, pp. 2239.
- DUNGEY, J. W. (1961) Interplanetary magnetic field and the auroral zones. *Phys. Res. Lett.*, v. 6, pp. 47.
- CBIHARA, Y. and EJIRI, M. (2000) Simulation study on fundamental properties of the storm time ring current. *J. Geophys. Res.*, v. 105.A7, pp. 15, 843-15,859.
- FELDSSTEIN, Y. I., DREMUKHINA, L.A., LEVITIN, A. E., MALL, U., ALEXEEV, I. I. and KALEGAEV, V. V. (2003) Energetics of the magnetosphere during the magnetic storm. *J. Atm. Sol. Ter. Phys.*, v. 65, pp. 429-446.
- GONZALEZ, W. D., TSURUTANI, B. T., GONZALEZ, A. L. C., SMITH, E. J., TANG, F. and AKASOFU, S. I. (1989) Solar wind-magnetosphere coupling during intense magnetic storm (1978-1979). *J. Geophys. Res.*, v. 94, pp. 8835.
- GONZALEZ, W. D. and TSURUTANI, B. T. (1987) Criteria of interplanetary parameters causing intense magnetic storms (Dst < 100 nT). *Planet. Space Sci.*, v. 35, pp. 1101.
- JADHAV, G., ALEX, S. and LAKHINA, G.S. (2004) Some characteristics of Intense Geomagnetic Storms and their Energy budget. *J. Geophys. Res.*, communicated.
- KAMIDE, Y., N., YOKOYAMA, W., GONZALEZ, B. T., TSURUTANI, I. A., DAGLIS, A., BREKKE, S. and MASUDA (1988) Two-step development of geomagnetic storms. *J. Geophys. Res.*, v. 103, pp. 6917.
- KLEIN, L.W. and BURLAGA, L.F. (1982) Magnetic clouds at 1 AU. *J. Geophys. Res.*, v. 87, pp. 613.
- LAKHINA, G. S. and ALEX, S. (2002) Space weather research in India: An overview. *Indian J. Radio and Space Phys.*, 337-348, 2002.
- LIEMOHN, M. W., KOZYRA, J. U., JORDANOVA, V. K., KHAZANOV, G. V., THOMSEN, M. F. and CAYTON, T. E. (1999) Analysis of early phase ring current recovery mechanism during geomagnetic storms. *Geophys. Res. Lett.*, v. 26, pp. 2845-2848.

- MAC- MAHON, R. M and GONZALEZ, W .D (1997): Energetics during the main phase of geomagnetic superstorms, *J. Geophys Res.*, v. 102, A7, pp. 14,199-14 207
- PERREAULT, P. and AKASOFU, S. I.(1978) A study of magnetic storms, *Geophys J. R. Astron Soc.*, v . 54, pp. 547
- RAJARAM, G. DHAR, A. and KUMAR, S. (2001) :Response of geomagnetic variations and 30 MHz Riometer absorption at Indian Antarctic station Maitri to conditions of 'zero' and 'high' solar wind *Adv .Space Res.*, v. 28, pp. 1661-1667
- ROSTOKER, G (1997) Physics of magnetic storms, (In) B T Tsurutani, W.D Gonzalez, Y Kamide and J. K Arballo (Eds.) *Magnetic Storms Geophysical Monograph*, v. 98, AGU, Washington D C, pp. 149.
- SCKOPKE, N. (1966) A general relation between the energy of trapped particles and the disturbance field near the earth, *J. Geophys Res.* , v. 71, pp. 3125.
- SIBECK, N, LOPEZ, RE and ROELOF, EC (1991) Solar wind control of the magnetopause shape, location and motion *J Geophys Res.*, v 96, pp 5489 5495
- TSURUTANI, B T and GONZALEZ, WD (1997) The interplanetary causes of magnetic storms A review, (In) B T Tsurutani, W D Gonzalez, Y Kamide and J K Aiballo (Eds.) *Magnetic Storms. Geophys. Mpnograph* v. 98, AGU, Washington, D. C., pp 77-89.
- TSURUTANI, B.T, KAMIDE, Y. ARBALLO, J. K, GONZALEZ, W.D. and Lepping, R.P. (1999) Interplanetary causes of great and superintense magnetic storms, *Phys. Chem. Earth* , v. 24, pp 101
- TSURUTANI, B. T, GONZALEZ W. D, LAKHINA, G. S and ALEX, S. (2003): The extreme magnetic storm of 1-2 September 1859 *J. Geophys. Res.*, v. 108, A7, pp 1268.